A radical-anion chain mechanism following dissociative electron transfer reduction of the model prostaglandin endoperoxide, 1,4-diphenyl-2,3-dioxabicyclo[2.2.1]heptane

David C. Magri* and Mark S. Workentin*

The model prostaglandin endoperoxide, 1,4-diphenyl-2,3-dioxabicyclo[2.2.1]heptane (**3**), was investigated in *N*,*N*-dimethylformamide at a glassy carbon electrode using various electrochemical techniques. Reduction of **3** occurs by a concerted dissociative electron transfer (ET) mechanism. Electrolysis at −1.6 V yields 1,3-diphenyl-cyclopentane-*cis*-1,3-diol in 97% by a two-electron mechanism; however, in competition with the second ET from the electrode, the resulting distonic radical-anion intermediate undergoes a β-scission fragmentation. The rate constant for the heterogeneous ET to the distonic radical-anion is estimated to occur on the order of 2×10^7 s^{-1}. In contrast, electrolyses conducted at potentials more negative than −2.1 V yield a mixture of primary and secondary electrolysis products including 1,3-diphenyl-cyclopentane-*cis*-1,3-diol, 1,3-diphenyl-1,3-propanedione, *trans*-chalcone and 1,3-diphenyl-1,3-hydroxypropane by a mechanism involving less than one electron equivalent. These observations are rationalized by a catalytic radical-anion chain mechanism, which is dependent on the electrode potential and the concentration of weak non-nucleophilic acid. A thermochemical cycle for calculating the driving force for β-scission fragmentation from oxygen-centred biradicals and analogous distonic radical-anions is presented and the results of the calculations provide insight into the reactivity of prostaglandin endoperoxides.
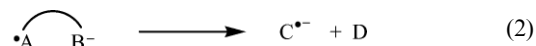
Introduction

Prostaglandin endoperoxides are biologically important compounds containing an O–O bond within a strained 2,3-dioxabicyclo[2.2.1]heptane ring structure.[1] In particular, the prostaglandin endoperoxide (PGH_2) is the immediate precursor to several classes of potent physiological regulators such as the prostaglandins, prostacyclins and thromboxanes.[2] At nanomolar concentrations, these physiological regulators have many profound effects including the activation of the inflammatory response, the sensation of pain, the regulation of blood pressure, the coagulation of blood, the induction of childbirth, and the regulation of the sleeping and waking cycle.[3]

One of the biochemical pathways of PGH_2, *via* the thromboxane synthase route, results in the formation of malondialdehyde (MDA) and 12-hydroxyheptadecatrienoic acid (HHT).[4] The mechanism is generally thought to result *via* β-scission fragmentation of alkoxyl radicals following cleavage of the O–O bond. One hypothesis is the mechanism is initiated by an inner-sphere electron transfer (ET) from an iron-heme centre of an enzyme.[2] It is also plausible that MDA and HHT may result from this type of dissociative ET to the O–O to yield a distonic radical-anion, a reactive intermediate possessing a spatially separated alkoxyl radical and alkoxyl anion, which may react *via* a β-scission fragmentation.[5–8]
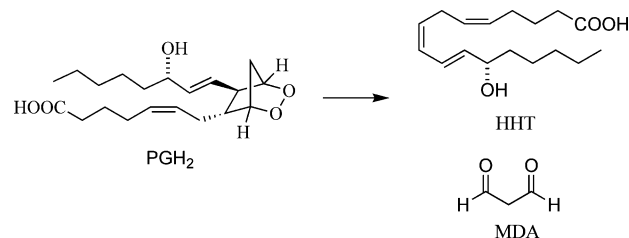

Radical-anions are gradually becoming accepted as biologically important species.[9] These reactive intermediates, possessing both a charge and radical character, typically result from the transfer of a single electron to a neutral molecule without any bonds breaking. With endoperoxides the electron is usually accepted into the σ* orbital largely associated with the O–O bond, which cleaves to yield the distonic radical-anion.[10] Most radical-anion rearrangements undergo a bond fragmentation that results in formation of a single species containing a spatially separated radical and anion [eqn (1)].[11–14] Recently, we reported an uncommon fragmentation, where a spatially separated radical-anion undergoes C–C bond fragmentation to yield a localized radical-anion and a neutral molecule [eqn (2)].[5]

$$[\overset{\frown}{A - B}]^{\bullet-} \longrightarrow {}^\bullet A \quad B^- \qquad (1)$$

$$\overset{\frown}{{}^\bullet A \quad B^-} \longrightarrow C^{\bullet-} + D \qquad (2)$$
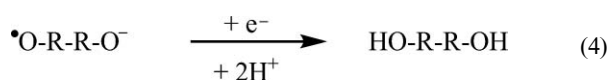
In that study, we reported the heterogeneous ET reduction of the bicyclic endoperoxides 1,4-diphenyl-2,3-dioxabicyclo[2.2.2]oct-5-ene (**1**) and 1,4-diphenyl-2,3-dioxabicyclo[2.2.2]octane (**2**).[5] Using

Department of Chemistry, The University of Western Ontario, London, Ontario, Canada N6A 5B7. E-mail: mworkent@uwo.ca; Fax: (+1) 519-661-3022; Tel: (+1) 519-661-2111 ext 86319

3354 | *Org. Biomol. Chem.*, 2008, **6**, 3354–3361

This journal is © The Royal Society of Chemistry 2008

electrochemical techniques we evaluated previously unknown kinetic and thermochemical data, delineated the reduction mechanism and provided insight into the fragmentation chemistry of neutral biradicals and analogous distonic radical-anions. Among many findings, we discovered that β-scission fragmentation of the distonic radical-anion from **2** initiates an unprecedented propagating radical-anion chain mechanism.
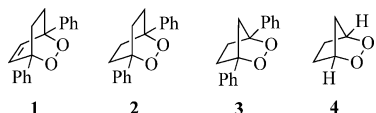
Thus far, we know of three common competing processes available to the distonic radical-anion after ET reduction of the O–O bond at an electrode: heterogeneous reduction, β-scission fragmentation, and *O*-neophyl (1,2-phenyl migration) fragmentation.[5–8,15–17] In all electrochemical studies to date the dominant pathway is reduction of the O–O bond to the distonic radical-anion [eqn (3)] followed by reduction and protonation to yield the *cis*-diol [eqn (4)]. However, in the electrochemical studies of various diphenyl-substituted endoperoxides, the distonic radical-anion undergoes a fragmentation reaction in competition with the second heterogeneous ET.[5–8]

$$R\text{-}O\text{-}O\text{-}R \xrightarrow{+ e^-} {}^\bullet O\text{-}R\text{-}R\text{-}O^- \quad (3)$$

$$^\bullet O\text{-}R\text{-}R\text{-}O^- \xrightarrow[+ 2H^+]{+ e^-} HO\text{-}R\text{-}R\text{-}OH \quad (4)$$

The fragmentation and rearrangement reactions of radical-anions are often assumed to be similar to neutral radicals. Recent work, mainly by Tanko and co-workers,[5,11,12] has provided evidence that this assumption is not valid as both charge and spin are contributing parameters governing the reactivity of radical-anion rearrangements. This distinction is of great importance considering many competing pathways, including disproportionation, reduction and fragmentation, result in the decomposition of prostaglandin endoperoxides. In particular, the bridgehead hydrogen atoms are vulnerable to base-induced decomposition.[18,19] As a consequence, compounds that are readily available, chemically stable and structurally simpler have routinely been used as models.[19,20] The common strategy has been to substitute the hydrogen atoms at the bridgehead carbons of the prostaglandin nucleus with phenyl rings, which prohibits base-induced disproportionation and greatly increases the stability.[18,21]

In this paper, we study the bicyclic endoperoxide 1,4-diphenyl-2,3-dioxabicyclo[2.2.1]heptane (**3**), as a model of a prostaglandin endoperoxide.[20–22] The compound was studied using a number of electrochemical techniques including cyclic voltammetry, convolution potential sweep voltammetry and preparative electrolysis in order to elucidate the ET reduction mechanism and evaluate previously unknown thermochemical parameters, notably the O–O bond dissociation energy and the standard reduction potential. The distonic radical-anion resulting from the concerted dissociative ET reduction of the O–O bond is observed to undergo a competing β-scission fragmentation with direct reduction from the electrode, and as observed previously with **2**, initiates a homogeneous propagating radical-anion chain mechanism. By exploiting the dual reactivity of the distonic radical-anion, we

provide an estimate of the rate constant for ET from the electrode. Furthermore, using a thermochemical cycle to calculate the driving force for β-scission fragmentation from oxygen-centred biradicals and analogous distonic radical-anions, including those derived from 2,3-dioxabicyclo[2.2.1]heptane (**4**) and PGH$_2$, we provide new insight into the reactivity of prostaglandin endoperoxides.

Results

Synthesis

Compound **3** was synthesized according to Scheme 1. Ethyl 3-benzoylpropionate from the esterification of 3-benzoylpropionic acid,[23] was reacted with acetophenone in dry toluene in the presence of excess sodium *tert*-butoxide at −78 °C. After 24 hours the solution was extracted with water and warmed at 70 °C resulting in the *in situ* loss of CO$_2$ and precipitation of 1,4-diphenyl-1,3-cyclopentadiene. Photo-oxygenation of the diene by irradiation of O$_2$ saturated solutions of 1 : 1 benzene–dichloromethane, containing a catalytic amount of *meso*-tetraphenylporphyrin (MTTP), afforded 1,4-diphenyl-2,3-dioxabicyclo[2.2.1]hept-5-ene.[24,25] The saturated endoperoxide, **3**, was prepared from the reduction of 1,4-diphenyl-2,3-dioxabicyclo[2.2.1]hept-5-ene with excess diimide generated *in situ* from potassium azodicarboxylate in the presence of acetic acid.[22,26] The final product **3** was recrystallized from ethanol as a crystalline white solid. The spectroscopic characterization can be found in the Experimental section.
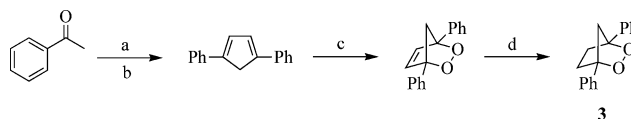

Scheme 1 The synthetic route and conditions used in the synthesis of the bicyclic diphenyl-substituted endoperoxide **3**. (a) NaO*t*Bu, toluene, −78 °C (b) ethyl 3-benzoylpropionate; Δ (c) O$_2$, MTTP, *hv*, 1 : 1 benzene–CH$_2$Cl$_2$ (d) N$_2$H$_2$, CH$_2$Cl$_2$.
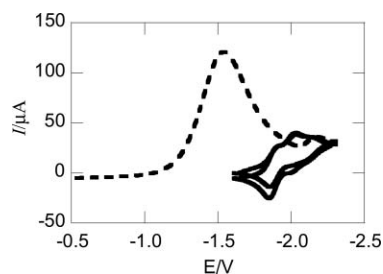
Cyclic voltammetry

The electrochemical reduction of 1,4-diphenyl-2,3-dioxabicyclo[2.2.1]heptane was studied by cyclic voltammetry using a glassy carbon electrode in *N*,*N*-dimethylformamide (DMF) containing 0.10 M tetraethylammonium perchlorate (TEAP). The voltammogram of **3**, as shown in Fig. 1, is characterized by an electrochemically irreversible cathodic peak at all scan rates investigated between 0.1 to 50 V s^{-1}.

The peak potential, E_p, at 0.1 V s^{-1} is located at −1.34 V *versus* SCE. At slow scan rates the peak width at half height, $\Delta E_{p/2} = E_{p/2} - E_p$ is uncharacteristically narrow with a peak width of 116 mV at 0.1 V s^{-1}. Increasing the scan rate, v, is found to shift the E_p negatively by 132 mV per log decade, resulting in the cathodic wave broadening up to 187 mV at 10 V s^{-1}. The transfer coefficient determined from the peak widths using $a = 1.857RT/(F\Delta E_{p/2})$ are found to decrease with v from 0.41 to 0.26. From the scan rate dependence of the peak potential and $a = 1.15RT/F[dE_p/(d\log v)]$, an average a of 0.23 is determined. The a values are consistent with a concerted dissociative ET mechanism.[27,28] On scanning back after the forward reduction in the positive direction, poorly defined
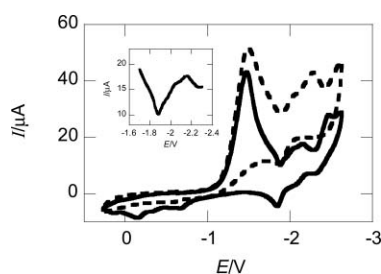
Fig. 1 Cyclic voltammograms of 1.7 mM of **3** in DMF containing 0.10 M TEAP in the absence (solid line) and presence (dashed line) of 10 equivalents of 2,2,2-trifluoroethanol at 0.2 V s^{-1}. The inset highlights the oxidative dip in the absence of acid.

anodic peaks are observed between 0 and -0.8 V presumably due to oxidation of the dialkoxide anion.[15] When the switching potential is extended past the end of the initial wave, which is normally dictated exclusively by diffusion, an oxidative dip is observed at -1.9 V. This feature of the voltammograms is most noticeable at slower scan rates. Following the dip at more negative scanned potentials there are other cathodic and anodic peaks attributed to products resulting from the electrochemical reduction of the **3**. Repetitive cycling voltammetry was used to probe the peaks in the vicinity of the dip as shown in Fig. 2. Two redox couples are observed at -1.83 V and -2.00 V.

Fig. 2 Cyclic voltammograms of 2.1 mM of **3**. The dashed-line is the initial reduction of the endoperoxide, followed by repetitively cycling through the redox couples twice between the switching potentials of -1.6 and -2.3 V at 1.0 V s^{-1}.

A striking observation is that on addition of weak non-nucleophilic acids there is a significant change in the voltammetry, notably the initial dissociative wave, as illustrated by the dashed line in Fig. 1. Table 1 compares the diagnostic voltammetry parameters for the initial wave with and without excess acid. Weak acids were chosen that are not electroactive within the potential range investigated. In the presence of 5 equivalents of a non-nucleophilic proton donor, such as 2,2,2-trifluoroethanol (TFE) or acetanilide, the initial wave is much broader with a peak width of 183 mV, the latter corresponding to an a value of 0.26. A 10% increase in the peak height, I_p is also observed. Addition of more than five equivalents of TFE has no additional effect on the initial peak height, while the peaks beyond the dissociative wave continue to increase. Furthermore, in the presence of excess acid the oxidative dip is not observed even at the slower scan rates. It should be emphasized that reduction of the acid does not occur within the potential window, and therefore, does not directly contribute to the observed increase in peak current values.

Table 1 Cyclic voltammetry data for the dissociative ET reduction of 1,4-diphenyl-2,3-dioxabicyclo[2.2.1]heptane in 0.10 M TEAP–DMF at 25 °C measured at a glassy carbon electrode

	v/V s^{-1}	**3**	**3** (acid)[c]
E_p/V[a]	0.1	-1.34	-1.50
	1.0	-1.52	-1.61
	10	-1.64	-1.73
$\Delta E_{p/2}$/mV	0.1	116	183
	1.0	167	198
	10	187	222
$a = 1.857RT/F\Delta E_{p/2}$	0.1	0.41	0.26
	1.0	0.29	0.24
	10	0.26	0.22
$a = 1.15RT/F(dE_p/d\log v)$		-132	-116
$(dE_p/d\log v)$/mV^{-1b}		0.23	0.25
n @ -1.6 V (no acid)		1.97	na[d]
n @ -1.6 V (acid)		na[d]	1.92
n @ -2.5 V		0.8	nd[d]

[a] Potentials are referenced *versus* ferrocene (0.475 V) *versus* SCE. [b] Based on scan rates between 0.1 and 10 V s^{-1}. [c] 10 mM 2,2,2-trifluoroethanol. [d] na = not applicable, nd = not determined.

## Constant potential electrolyses

At the potentials between -1.5 and -2.0 V in the absence of acid, **3** consumes 1.97 mole equivalents of charge. The major product is the *cis*-diol, 1,3-diphenyl-cyclopentane-1,3-*cis*-diol in 97% yield. In the presence of TFE, 1.92 F mol^{-1} of charge is consumed, however the yield of *cis*-diol is quantitative. In contrast, electrolysis at -2.5 V with no additional acid results in coulometric values of only 0.8 F mol^{-1} charge consumed, and the appearance of electroactive products at the expense of the dissociative wave. Work-up of the electrolysis mixture revealed several products by gas chromatography, as shown in Scheme 2, including *cis*-diol (35%), 1,3-diphenyl-1,3-propanedione (10%), *trans*-chalcone (15%) and 1,3-diphenyl-1,3-hydroxypropane (40%) All compounds were confirmed by mass spectrometry.
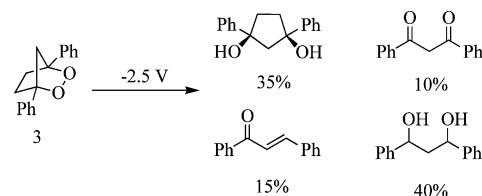
Scheme 2 The products and yield from the reduction of **3** at -2.5 V.

Heterogeneous kinetics and thermochemical parameters

The heterogeneous ET kinetics and thermochemical parameters for reduction of the O–O bond were evaluated by convolution potential sweep voltammetry as shown in Fig. 3.[29] The experiments were performed in the presence of excess weak acid as this made the voltammetry more reproducible. Only scan rates of 1.0 V s^{-1} and faster were usable because of non-Cottrell behaviour at the slower scan rates, which results in lower limiting currents. A total of 11 background-subtracted cyclic voltammograms were recorded between 1.0 and 20 V s^{-1}. The background subtracted i–E curves were transformed into sigmoidal-shaped I–E curves by use of the convolution integral,[29,30] and found to be in good agreement with an error less than 3%. From the limiting currents, I_{lim}, and the
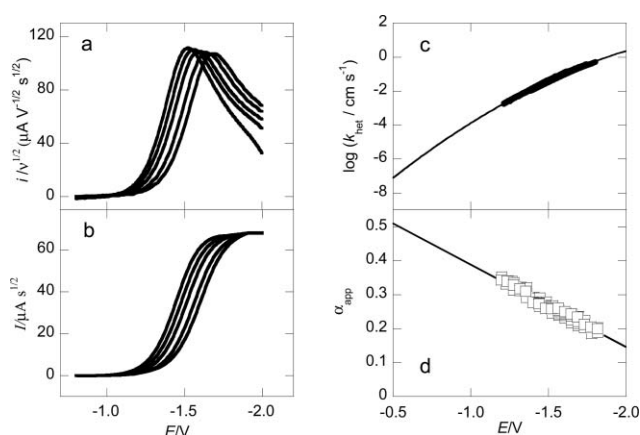
Fig. 3 (a) Background-subtracted linear sweep voltammograms of 1.8 mM of **3** in DMF containing 0.10 mol L^{-1} TEAP (from left to right: 1.0, 2.0, 4.0, 10, 20 V s^{-1}); (b) the convolution curves as a function of scan rate (c) overlapping potential dependence of the log k_{het} and (d) the potential dependence of a_{app} at 10 scan rates between 1.0 and 20 V s^{-1}.

known area of the glassy carbon electrode, the diffusion coefficient in the presence of 0.1 M TEAP was determined to be 6.5 × 10^{-6} cm^2 s^{-1}. From the potential dependence of a for a concerted dissociative ET mechanism (Fig. 3d), the E°_{diss} was determined by extrapolation of the a–E data to $a = 0.5$, and the intrinsic barrier, $\Delta G_o^{\neq}$, was determined from the slope of the linear regression.

In Table 2 the parameters determined from the convolution analysis are summarized. As determined from the a–E plot, the evaluated E°_{diss} and $\Delta G_o^{\neq}$ of **1** are −0.54 V and 11.8 kcal mol^{-1}, respectively. The E°_{diss} is substantially more positive than the E_p by over 0.8 V. The large overpotential observed in the cyclic voltammograms is attributed to the large $\Delta G_o^{\neq}$ that must be overcome to stretch and break the O–O bond. The log k°_{het} is considerably low with a value of −6.8 consistent with a totally irreversible rate-determining electrode reaction characteristic of concerted dissociative ET. The accuracy of the evaluated thermochemical parameters in acidic media were adequately reproduced by digital simulation of the dissociative waves using the data in Tables 1 and 2 for a two-electron concerted dissociative mechanism.

Table 2 Data acquired by convolution sweep potential voltammetry of **3** in 0.10 mol L^{-1} TEAP–DMF at 25 °C at a glassy carbon electrode

D^a/cm^2 s^{-1}	6.5 × 10^{-6}
$E^\circ_{diss}{}^b$/V	−0.54
log (k°_{het}/cm s^{-1})^c	−6.8
$\Delta G_o^{\neq d}$/kcal mol^{-1}	11.8
$\lambda_{het}{}^e$/kcal mol^{-1}	18
BDE^g/kcal mol^{-1}	20
BDFE^h/kcal mol^{-1}	10

^{a} Determined from the convoluted limiting current and the area of the electrode using ferrocene with a diffusion coefficient 1.13 × 10^{-5} cm^2 s^{-1}. ^{b} Estimated error is ±0.10 V and uncorrected for the double layer. ^{c} Obtained by interpolation of the heterogeneous kinetics from a quadratic fit at E°_{diss}. Estimated error of ± 0.5 from digital simulation. ^{d} $\Delta G_o^{\neq}$ determined from the slope of a_{app} vs. E plots and $\Delta G_o^{\neq} = F/[8(da/dE)]$. ^{e} $\lambda_{het} = 55.7/r_{eff}$; the calculated radius r_{AB} of 4.6 Å was determined from the Stokes–Einstein equation and the diffusion coefficient. ^{f} Effective radius of 3.0 Å from $r_{eff} = r_B(2r_{AB} − r_B)/r_{AB}$. ^{g} $\Delta G_o^{\neq} = (BDE + \lambda_{solvent} + \lambda_{inner})/4$ with $\lambda_{inner} = 9$ kcal mol^{-1}. ^{h} BDFE = 23.06($E^\circ_{\cdot ORRO-} − E^\circ_{diss}$).

The E°_{diss} is related to the O–O bond dissociation energy (BDE) by the equation $E^\circ_{diss} = E^\circ_{\cdot ORRO-} − BDFE/F$ derived from a thermochemical cycle where $E^\circ_{\cdot ORRO-}$ is the reduction potential of the distonic radical-anion, F is the Faraday constant and the BDFE is the bond dissociation free energy, which is the BDE corrected for entropy (BDFE = BDE − $T\Delta S$).[10,31] The $E^\circ_{\cdot ORRO-}$ was approximated from the standard potential of the cumyl alkoxyl radical equal to −0.12 V.[32] Using the equation based on E°_{diss} the BDFE is 10 kcal mol^{-1}.

The BDE was determined using Savéant's concerted dissociative ET model[27,28] from the experimental $\Delta G_o^{\neq}$ and the expression $\Delta G_o^{\neq} = (BDE + \lambda_{solvent} + \lambda_{inner})/4$ where $\lambda_{solvent}$ is the solvent reorganization energy and λ_{inner} is the inner reorganization energy due to changes in the bond lengths and bond angles. An effective radius approach was used to account for solvation of only the portion of the molecule receiving the charge, while the rest of the molecule acts to shield the charge from the solvent.[33] The empirical relation $\lambda_{solvent} = 55.7/r_{eff}$ was used where $\lambda_{solvent}$ is given in kcal mol^{-1} and r_{eff} is the effective molecular radius, given in Å.[27] r_{eff} is equal to 3.0 Å resulting in $\lambda_{solvent}$ equal to 18 kcal mol^{-1}. Using the $\lambda_{solvent}$ value (temporarily assuming $\lambda_{inner} = 0$) the BDE would be 29 kcal mol^{-1}.
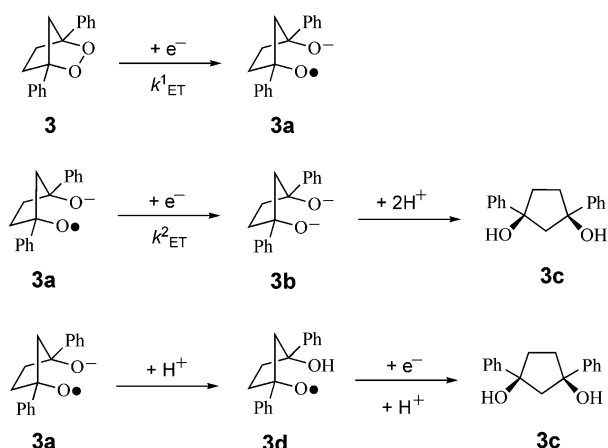
A comparison of the kinetic and thermodynamic parameters of **3** with our previous studies of **1** and **2** reveals some interesting trends. The standard heterogeneous rate constant, k°_{het}, and standard reduction potential, E°_{diss}, are identical within experimental error. The diffusion coefficient of **3** is slightly lower as might be expected for a carbon skeleton one methylene unit less. However, there is one noticeable difference. The intrinsic barrier of **3** is much larger suggesting a BDE of 29 kcal mol^{-1} compared to the average value of 20 kcal mol^{-1} determined for **1** and **2**.[5] This difference may be attributed to a significant λ_{inner} contribution from the relief of strain upon fragmentation of the O–O within the bicyclo[2.2.1]heptane framework. The λ_{inner} is often assumed to be negligible with respect to the magnitude of the BDE.[27] However, the BDE in endoperoxides are rather small. Considering the BDE of **3** is expected to be similar to **1** and **2** on the order of 20 kcal mol^{-1}, λ_{inner} may contribute 9 kcal mol^{-1} to the intrinsic barrier.

Discussion

The voltammetry of **3** is consistent with reduction of the O–O bond by a concerted dissociative ET mechanism, where fragmentation occurs simultaneously with electron uptake [eqn (3)]. At a potential of −1.5 V, the major product is the corresponding 1,3-diphenyl-cyclopentane-cis-1,3-diol in 97% yield. However, at more negative potentials, in addition to the cis-diol, a number of other compounds are identified: 1,3-diphenyl-1,3-propanedione, trans-chalcone and 1,3-diphenyl-1,3-hydroxypropane.

Scheme 3 depicts the ET reduction mechanism of **3** considering the electrode is the only electron source and in the absence of the competing β-scission fragmentation, which accounts for the majority of the 97% yield of 1,3-diphenyl-cyclopentane-cis-1,3-diol. The near quantitative formation of the cis-diol **3c**, results in the consumption of two electrons per molecule. The first electron is accepted into an σ* orbital mainly localized on the O–O bond, which in concert cleaves resulting in the formation of the distonic radical-anion **3a** with a negative charge on one oxygen atom and an unpaired electron on the other. Subsequently, **3a** generated in

This journal is © The Royal Society of Chemistry 2008

*Org. Biomol. Chem.*, 2008, **6**, 3354–3361 | 3357

Scheme 3 The major mechanistic pathways for formation of 1,3-diphenyl-cyclopentane-1,3-*cis*-diol **3c** by reduction of **3** at a glassy carbon electrode.

the vicinity of the electrode, could be reduced to the dialkoxide **3b** before diffusing away from the electrode, and then protonated in the reaction solution or upon work-up to yield **3c**. Alternatively, **3a** could be protonated by a weak acid to yield the alkoxyl radical **3d**, which could be further reduced by the electrode before subsequently being protonated to yield **3c**. Either route from **3a** yields a near quantitivative amount of **3c**. Due to electrostatic interactions, the reduction potential of **3a** is likely to be slightly more negative than **3d**, the latter is easily approximated to have a value similar to the cumyl alkoxyl radical with a standard potential of -0.12 V *versus* SCE in DMF.[32] However, with the E_p located at a potential of -1.5 V, the reduction of both **3a** and **3d** are predicted to be thermodynamically favorable by at least 30 kcal mol^{-1}.

The proposed ET reduction mechanism of **3**, including the β-scission fragmentation, is depicted in Scheme 4. To account for the experimental observations, including the formation
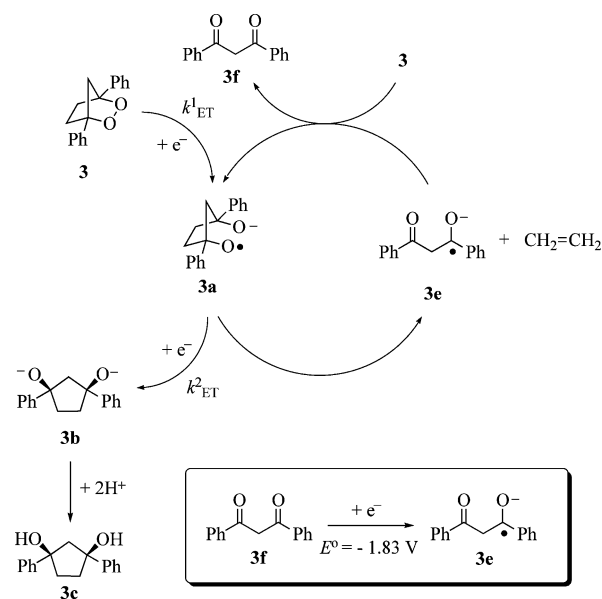
of 1,3-diphenyl-cyclopentane-*cis*-1,3-diol and 1,3-diphenyl-1,3-propanedione, a radical-anion chain mechanism is postulated.[5,7] Scheme 4 depicts two of the possible fates for **3a**. As already mentioned with respect to Scheme 3, the predominant pathway, occurring in the vicinity of the electrode, is reduction of **3a** to the dialkoxide **3b**, which is protonated in solution or upon work-up to yield the *cis*-diol **3c**. Alternatively, **3a** could be protonated in the reaction media, by 1,3-diphenyl-1,3-propanedione or upon addition of an external acid, to yield the alkoxyl radical **3d**, which could be further reduced and subsequently protonated to yield **3c**.

The formation of 1,3-diphenyl-1,3-propanedione, a product with a lower molecular weight than the endoperoxide, results from the β-scission fragmentation of **3a**, which competes with reduction from the electrode. The proposed mechanism in Scheme 4 also accounts for the observed dip after the dissociative wave, the affect of excess weak acid and the potential dependence on the electron stoichiometry.

At a potential of -1.6 V, 3% of **3a** reacts by a competitive β-scission fragmentation to yield **3f** and ethylene *via* formation of the ketyl radical **3e**, a radical-anion with the spin and charge no longer spatially separated. The radical-anion **3e**, formed as a consequence of the fragmentation, is a potential homogeneous ET donor capable of reducing **3**. The standard potential of 1,3-diphenyl-1,3-propanedione **3f** was measured to be -1.83 V *versus* SCE as illustrated in Fig. 2. This is 1.3 V more negative than the E°_{diss} of **3**. Therefore, the homogeneous reduction of **3** and **3a** are both thermodynamically favourable by 30 kcal mol^{-1}.

In Fig. 1 the cyclic voltammogram displays an oxidative dip after the dissociative wave rather than a gradual decrease in current dictated exclusively by diffusion. The dip occurs just after the standard potential of **3f** at -1.83 V. This feature in the voltammogram, most noticeable at slower scan rates, is a consequence of the competitive β-scission fragmentation. The sudden drop in current reflects a decrease in the amount of **3** diffusing towards the electrode as the endoperoxide is intercepted by **3e** and homogeneously reduced to generate **3a** and **3f**. Any **3f** could be reduced by the electrode surface and react with more incoming **3** thus propagating a chain reaction.

As shown in Scheme 5, excess weak acid affects the reduction mechanism of **3** in two ways: i) by protonation of the distonic radical-anion **3a** and ii) by protonation of the radical-anion **3e**. In the first case, the electrolyses of **3** in the presence of 10 mM TFE at potentials between -1.4 to -1.8 V, no **3f** was detected. The only isolated product was the *cis*-diol **3c**. This observation suggests that protonation of **3a** hinders the β-scission fragmentation of the alkoxyl radical **3d** so that reduction from the

Scheme 4 The propagating radical-anion chain mechanism proposed for the ET reduction of **3**. 1,3-diphenyl-1,3-propanedione **3f** acts as a homogeneous electron donor at a reduction potential of -1.83 V.
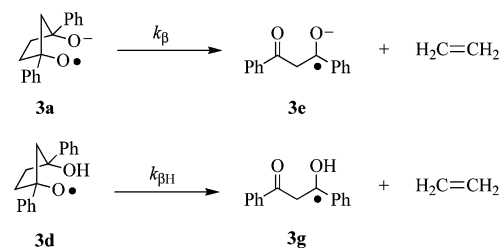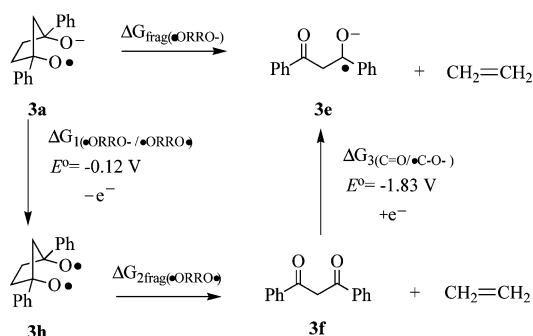

Scheme 5 β-Scission fragmentation of the distonic radical-anion **3a** to the radical-anion **3e** fragments faster than the alkoxyl radical **3d** to the carbon radical **3g**.

electrode is quantitative. This observation supports the hypothesis that both charge and spin affect the rates of radical-anion rearrangements.[11,12] The β-scission fragmentation of the alkoxyl radical **3d** must, therefore, be slower than β-scission fragmentation of the distonic radical-anion **3a**. Excess acid also affects the reduction mechanism by protonating the radical-anion donor **3e**, which prevents homogeneous reduction of **3**.

The applied potential also plays a role on the reduction mechanism of **3**. At potentials between −1.4 V and −2.0 V, approximately 2 F mol⁻¹ of charge is consumed during the electrolysis. However, at −2.5 V only 0.8 F mol⁻¹ of charge is required for complete reduction of the endoperoxide. The reasoning for this difference in the charge consumption can be explained by the propagating radical-anion chain mechanism shown in Scheme 4. The distonic radical-anion **3a** can either be reduced to the dialkoxide or fragment to yield radical-anion **3e**, which can act as a homogeneous ET donor to **3** yielding **3f** and another molecule of **3a**. For every **3a** generated, one molecule of **3f** can theoretically result to propagate the catalytic cycle. However, 1,3-diphenyl-1,3-propanedione **3f** is not a robust catalyst as it could be reduced to the radical-anion **3e** and then protonated by the alpha protons of **3f** by a competing self-protonation mechanism.[34] However, at an applied potential of −2.5 V both aryl ketones could be reduced to yield the dianion, which can act as a two-electron donor, which inhibits the self-protonation mechanism provided the heterogeneous ET to the radical-anion **3e** is faster than the proton transfer from **3f**. Efficient propagating chain reactions with stable homogeneous donors require only 0.1 F mol⁻¹ of charge.[7,35,36] The competing reduction and self-protonation mechanisms of **3f** contribute to the higher electron stoichiometry of 0.8 F mol⁻¹ at −2.5 V as we similarly observed with **2**.[5]

Thermochemical cycle

Scheme 6 illustrates a thermochemical cycle that identifies three parameters contributing to the driving force for fragmentation of the distonic radical-anion:[13] (i) the thermodynamic stability of the delocalized distonic radical-anion as measured by the oxidation potential of the biradical, (ii) the fragmentation of the biradical, and (iii) the stability of the localized radical-anion as measured by the reduction potential.

Scheme 6 Thermochemical cycle for evaluating the driving force for fragmentation of the distonic radical-anion **3a**.

To simplify the approach, no correction has been made to account for any possible interaction between the radical and anion portions of the distonic radical-anion. From the thermochemical

Table 3 Thermodynamic data for fragmentation of neutral biradicals and distonic radical-anions of select endoperoxides including PGH₂

Thermochemical parameters	2^a	3	4	PGH₂
$\Delta H^\circ_{\text{f(ROOR)}}{}^b$	12.60	29.1	−16.1	−161.3
$\Delta S^\circ_{\text{(ROOR)}}{}^b$	85.19	77.15	25.08	198.6
$\Delta G^\circ_{\text{f(ROOR)}}$	−12.8	6.1	−23.6	−220.5
BDFE	9.0	10.0	23.0^d	23.0^d
$\Delta G^\circ_{\text{f(}^\bullet\text{ORRO}^\bullet)}{}^e$	−3.8	16.1	−0.6	−197.5
$\Delta G^\circ_{\text{f(diketone)}}{}^b$	−73.4	−68.2	−89.6	−89.6
$\Delta G_{2\text{frag(}^\bullet\text{ORRO}^\bullet)}{}^f$	−73.1	−87.8	−92.5	−98.0
$\Delta G_{1(^\bullet\text{ORRO}^-/^\bullet\text{ORRO}^\bullet)}{}^g$	−2.8	−2.8	−4.6	−4.6
$\Delta G_{3(\text{C=O}/^\bullet\text{C-O}^-)}{}^h$	−45.4	−42.2	−69	−69
$\Delta G_{\text{frag(}^\bullet\text{ORRO}^-)}{}^i$	−30.5	−48.4	−28.1	−33.6

a From reference 5. *b* Values at 298 K in kcal mol⁻¹ except for $\Delta S^\circ_{\text{(ROOR)}}$ in cal K⁻¹ mol⁻¹; group additivity estimates from the NIST Structures and Properties Database, reference 37. *c* Estimated from reference 37 using hydrocarbon models without O atoms and corrected using values from reference 38. *d* BDFE = $23.06(E^\circ_{\cdot\text{ORRO}^-} - E^\circ_{\text{diss}})$; E°_{diss} from reference 6. $E^\circ_{\cdot\text{ORRO}^-}$ approximated as −0.20 V for **4** and PGH₂ from reference 32. *e* $\Delta G^\circ_{\text{f(}^\bullet\text{ORRO}^\bullet)}$ = BDFE + $\Delta G^\circ_{\text{f(ROOR)}}$. *f* Free energy for fragmentation of the biradical: $\Delta G_{2\text{frag(}^\bullet\text{ORRO}^\bullet)}$ = $\Delta G^\circ_{\text{f(diketone)}}$ + $\Delta G^\circ_{\text{f(alkene)}}$ − $\Delta G^\circ_{\text{f(}^\bullet\text{ORRO}^\bullet)}$; $\Delta G^\circ_{\text{f(alkene)}}$: $\Delta G^\circ_{\text{f(ethylene)}}$ = −3.5 kcal mol⁻¹; $\Delta G^\circ_{\text{f(HHT)}}$ = −205.9 kcal mol⁻¹; from reference 37. *g* $\Delta G_{1(^\bullet\text{ORRO}^-/^\bullet\text{ORRO}^\bullet)}$ = $FE_{1(^\bullet\text{ORRO}^-/^\bullet\text{ORRO}^\bullet)}$; $E_{1(^\bullet\text{ORRO}^-/^\bullet\text{ORRO}^\bullet)}$ estimated from the value for the cumyloxy radical $E^\circ_{\cdot\text{ORRO}^-}$ = −0.12 V; $E^\circ_{\cdot\text{ORRO}^-}$ = −0.20 V reference 32. *h* $\Delta G_{3(\text{C=O}/^\bullet\text{C-O}^-)}$ = $-nFE_{(\text{C=O}/^\bullet\text{C-O}^-)}$; $n = 1$, $E_{2(\text{C=O}/^\bullet\text{C-O}^-)}$ = −1.97 V; $E_{3(\text{C=O}/^\bullet\text{C-O}^-)}$ = −1.83 V; $E_{4(\text{C=O}/^\bullet\text{C-O}^-)}$ = −3.0 V. *i* $\Delta G_{\text{frag(}^\bullet\text{ORRO}^-)}$ = $\Delta G_{1(^\bullet\text{ORRO}^-/^\bullet\text{ORRO}^\bullet)}$ + $\Delta G_{2\text{frag(}^\bullet\text{ORRO}^\bullet)}$ − $\Delta G_{3(\text{C=O}/^\bullet\text{C-O}^-)}$.

cycle, the overall driving force for the fragmentation of the distonic radical-anion $\Delta G_{\text{frag(}^\bullet\text{ORRO}^-)}$ is given by eqn (5):

$$\Delta G_{\text{frag(}^\bullet\text{ORRO}^-)} = \Delta G_{1(^\bullet\text{ORRO}^-/^\bullet\text{ORRO}^\bullet)} + \Delta G_{2\text{frag(}^\bullet\text{ORRO}^\bullet)} - \Delta G_{3(\text{C=O}/^\bullet\text{C-O}^-)} \quad (5)$$

The $\Delta G_{1(^\bullet\text{ORRO}^-/^\bullet\text{ORRO}^\bullet)}$ and $\Delta G_{3(\text{C=O}/^\bullet\text{C-O}^-)}$ values are calculated from the oxidation potential of the distonic radical-anion and the reduction potential of the ketone, respectively, from electrochemically measurements or literature values.[32] For $\Delta G_{2\text{frag(}^\bullet\text{ORRO}^\bullet)}$ we also require the Gibbs energies of formation of the biradical. It was calculated according to eqn (6)

$$\Delta G_{2\text{frag(}^\bullet\text{ORRO}^\bullet)} = \Delta G^\circ_{\text{f(diketone)}} + \Delta G^\circ_{\text{f(alkene)}} - \Delta G^\circ_{\text{f(}^\bullet\text{ORRO}^\bullet)} \quad (6)$$

where $\Delta G^\circ_{\text{f(diketone)}}$, $\Delta G^\circ_{\text{f(alkene)}}$ and $\Delta G^\circ_{\text{f(}^\bullet\text{ORRO}^\bullet)}$ are the Gibbs free energies for the diketone, alkene and the biradical, respectively. The Gibbs free energy for the biradical was calculated from the free energy of the endoperoxide,[37,38] and the experimentally determined BDFE according to $\Delta G^\circ_{\text{f(}^\bullet\text{ORRO}^\bullet)}$ = BDFE + $\Delta G^\circ_{\text{f(ROOR)}}$. Table 3 summarizes the thermochemical values pertaining to the previously studied diphenyl endoperoxide **2**,[5] and new data for **3**, **4** and PGH₂.

The enthalpies and entropies in Table 3 are directly from the NIST database.[37] The $\Delta H^\circ_{\text{f(ROOR)}}$ of the bridgehead diphenyl-substituted endoperoxides **2** and **3** are positive values in contrast to the unsubstituted endoperoxides **4** and PGH₂, which are negative, while the $\Delta S^\circ_{\text{(ROOR)}}$ tends to increase with the number of atoms and degrees of freedom within each molecule. The $\Delta G^\circ_{\text{f(ROOR)}}$ of **3** is a positive value in contrast to the other three endoperoxides, whereas the $\Delta G^\circ_{\text{f(ROOR)}}$ of PGH₂ is an order of magnitude more negative than **2** and **4**. Comparison of the $\Delta G^\circ_{(^\bullet\text{ORRO}^\bullet)}$ for **3** and PGH₂ predicts correctly that phenyl rings at the bridgehead positions provide stability to the strained 2,3-dioxabicyclo[2.2.1]heptane ring structure.[18,21]

From eqn (5), based on the thermochemical cycle in Scheme 6, the calculated $\Delta G_{\text{frag}(\bullet \text{ORRO}-)}$ for **3a** is -48.4 kcal mol^{-1} in agreement with the observed β-scission fragmentation from the distonic radical-anion. Similarly, $\Delta G_{\text{frag}(\bullet \text{ORRO}-)}$ for **4** and PGH$_2$ are -28.1 and -33.6 kcal mol^{-1} suggesting that β-scission fragmentation from their corresponding distonic radical-anions is also thermodynamically favourable. From eqn (6), the $\Delta G_{\text{2frag}(\bullet \text{ORRO}\bullet)}$ for the biradicals of **2** and **3** are favourable with values of -73.1 and -87.8 kcal mol^{-1}. This is consistent with the observed β-scission fragmentation products from the thermolysis and photolysis of saturated bicyclic endoperoxides.[1,39] The calculations also reveal that the driving force for biradical β-scission fragmentation from **4** and PGH$_2$, with values of -92.5 and -98.0 kcal mol^{-1}, is also thermodynamically favourable. For all the endoperoxides examined, both the oxygen-centred biradicals and distonic radical-anions are predicted to react *via* β-scission fragmentation pathways.

The elaborate reduction mechanism deterred us from determining the rate constant for β-scission fragmentation of the distonic radical-anions **3a** using digital simulation. Rather we used the β-scission fragmentation of the cumyl alkoxyl radical, with a known rate constant of 7×10^5 s^{-1}, as a starting reference point.[40] This value is thought to represent the lower limit for fragmentation of **3a**. The known quantity of 1,3-diphenyl-1,3-propanedione formed during the heterogeneous ET reduction can be exploited in order to estimate the rate constant for ET to **3a**. Using the experimental product ratio of 97 : 3 [*cis*-diol **3c** : 1,3-diphenyl-1,3-propanedione **3f**] and 7×10^5 s^{-1} for k_β, the ET rate constant is estimated to occur with a rate constant of 2×10^7 s^{-1}, which is the same as that observed with 1,4-diphenyl-2,3-dioxabicyclo[2.2.2]octane with a value of 3×10^7 s^{-1}.

Conclusions

The strained bicyclic endoperoxide 1,4-diphenyl-2,3-dioxabicyclo-[2.2.1]heptane (**3**) was studied as a representative model of a prostaglandin endoperoxide using heterogeneous electrochemical techniques. Reduction of the O–O bond occurs by a dissociative ET mechanism with thermodynamic and kinetic parameters consistent with our previous findings with other endoperoxides that the kinetics are slow and the O–O bond is weak. However, one noticeable distinction is that the intrinsic barrier includes a significant inner reorganization energy contribution attributed to the relief of ring strain. An interesting observation from the thermochemical cycle in Scheme 6 and the data in Table 3 is that fragmentation of distonic radical-anions are calculated to be thermodynamically favourable. The thermochemical calculations suggest that in many respects **3** is an appropriate model for PGH$_2$.

This study also highlights another rare example of a radical-anion chain mechanism initiated by the concerted dissociative ET reduction of a bicyclic endoperoxide.[5] Reduction of **3** yields a distonic radical-anion **3a** that undergoes a β-scission fragmentation in competition with ET reduction from the electrode. The fragmentation results in the formation of ethylene and the ketyl radical-anion **3e**, which reduces the endoperoxide, thus propagating a homogeneous radical-anion chain mechanism. However, a competing self-protonation mechanism involving 1,3-diphenyl-1,3-propanedione decreases the efficiency of the radical-anion chain reaction. Nonetheless, the significance of this uncommon mechanism should not be underestimated. In collaboration, we recently reported the first example of a competitive concerted-stepwise dissociative ET mechanism for antimalarial G3-factor endoperoxides,[41] which potentially opens up an alternative mode of action. Novel endoperoxides that react by a radical-anion chain mechanism may be useful in designing antimalarial prodrug models.[42] Perhaps, homogeneous radical-anion chain mechanisms may also be an unrealized mechanistic pathway in the reactivity of prostaglandin endoperoxides.

Experimental

Materials

N,N-Dimethylformamide (DMF) was distilled over CaH$_2$ under a nitrogen atmosphere at reduced pressure. Tetraethylammonium perchlorate (TEAP) from Fluka was recrystallized three times from ethanol and stored under vacuum. Flash chromatography was performed with silica gel 60 (230–400 mesh ASTM) from EM science. Reactions were developed in the chosen eluant with Kieselgel 60 F$_{254}$ TLC plates and viewed by ultraviolet or visible light or iodine staining. Toluene was freshly distilled from sodium and benzophenone. Photo-oxygenation reactions were performed in solutions of spectroscopic grade dichloromethane (Caledon) and benzene (EM Science). Other solvents and reagents not specified were used without purification and obtained from Aldrich.

Instrumentation

Melting points were recorded on an Electrothermal 9100 capillary melting point apparatus and were corrected. UV-visible spectra were recorded on a Varian Cary 100 Bio UV-visible spectrometer. Infra-red spectra were recorded on a Bruker Vector 33 FT-IR spectrometer on NaCl plates or in a solution cell. The IR frequencies are reported in cm^{-1} and followed by a letter (w, m, or s) designating the relative strength of the IR stretches as weak, medium, or strong. Nuclear magnetic resonance spectra were recorded on a Varian Mercury spectrometer and are reported in ppm. ^{1}H and ^{13}C NMR spectra were recorded at 400.1 and 100.6 MHz, respectively, with CDCl$_3$ as the solvent. Spectra are reported in ppm *versus* tetramethylsilane ($\delta_H = 0.00$) for ^{1}H NMR and CDCl$_3$ ($\delta_C = 77.00$) for ^{13}C NMR. Mass spectrometry was performed on a MAT 8200 Finnigan high-resolution mass spectrometer by electron impact (EI) and by chemical ionization (CI) with isobutane.

Synthetic procedures

1,4-Diphenyl-2,3-dioxabicyclo[2.2.1]heptane. The target compound was synthesized from 1,4-diphenyl-1,3-cyclopentadiene[43,44] by photo-oxygenation to yield 1,4-diphenyl-2,3-dioxabicyclo-[2.2.1]heptene, which was reduced with potassium azodicarboxylate to yield the desired product. It was recrystallized from ethanol (110 mg, 34%) as white crystals. mp 110–112 °C; ν_{max}(NaCl)/cm^{-1}: 3055 m, 2984 w, 2944 w, 1604 w, 1497 w, 1450 m, 1340 m, 1267 m, 898 m, 742 s, 697 s; δ_H(400 MHz, CDCl$_3$, SiMe$_4$): 2.32–2.38(2H, m), 2.54–2.64 (2H, m), 2.72–2.78 (1H, m), 2.88–2.94 (1H, m), 7.33–7.43 (6H, m), 7.48–7.53 (4H, m); δ_C(100 MHz, CDCl$_3$, SiMe$_4$): 35.35, 52.70, 91.21, 126.59, 128.33, 128.49, 134.56; *m/z*(EI):

252(M$^{\bullet+}$, 8), 224(8), 220(22), 219(100), 115(6), 105(89), 91(15), 77(48), 51(15); Exact Mass: 252.1147 (calculated 252.1150).

Electrochemistry

Cyclic voltammetry was performed using either a Perkin-Elmer PAR 283, or 263A potentiostat interfaced to a personal computer equipped with PAR 270 electrochemistry software. The working electrode was a 3 mm diameter glassy carbon rod (Tokai, GC-20) sealed in glass tubing. The counter electrode was a 1 cm^2 Pt plate. The reference electrode was a silver wire immersed in a glass tube with a sintered end containing 0.10 M TEAP in DMF. After each experiment, it was calibrated against the ferrocene/ferricinium couple at 0.475 V *versus* KCl saturated calomel electrode (SCE) in DMF. Constant potential electrolyses were conducted with a 12 mm tipped glassy carbon rotating disk electrode (EDI101) with a CTV101 speed control unit from Radiometer Analytical. The experimental set-up was the same as previously reported.[5]

Heterogeneous electrolysis

From the electrolysis of 1,4-diphenyl-2,3-dioxabicyclo[2.2.1]-heptane at the peak potential was recovered 1,3-diphenyl-cyclo-pentane-*cis*-1,3-diol as a white solid in 97% yield; ν_{max}(NaCl)/cm^{-1}: 3375 s (broad), 3088 m, 3060 m, 3030 m, 2966 m, 2938 m, 2858 w, 1665 w, 1602 w, 1495 m, 1449 s, 1406 m, 1262 m, 1227 m, 1100 m, 1071 s, 878 m, 759 s, 700 s; δ_H(400 MHz, CDCl$_3$, SiMe$_4$): 2.42–2.57 (6H, m), 3.43 (2H, s, br), 7.25–7.31 (2H, m), 7.34–7.41 (4H, m), 7.50–7.55 (4H, m); alcohol peak verified by deuterium exchange; δ_C(100 MHz, CDCl$_3$, SiMe$_4$): 41.85, 55.83, 83.92, 124.94, 127.12, 128.36, 145.77; m/z(EI): 237(M − 17, 15), 236(M − 18, 41), 133(7), 105(100), 91(5), 77(13); m/z(CI): 238(20), 237(100), 236(42), 220(6), 219(39), 218(33), 177(6), 105(52), 77(7); Exact Mass: (M − 18) 236.1204 (calculated 236.1201).

Acknowledgements

Notes and references

1 *Organic Peroxides*, ed. W. Ando, John Wiley & Sons Ltd., New York, 1992.
2 C. Martin and V. Ullrich, in *Prostaglandins, Leukotrienes and other Eicosanoids: from Biogenesis to Clinical Applications*, ed. F. Marks and G. Fürstenberger, Wiley-VCH, Weinheim, New York, 1999, pp. 89–108.
3 D. J. Voet and J. G. Voet, *Biochemistry*, Wiley, Hoboken, NJ, 3rd edn, 2004.
4 J. P. Plastaras, F. P. Guengerich, D. W. Nebert and L. J. Marnett, *J. Biol. Chem.*, 2000, **275**, 11784–11790.
5 D. C. Magri and M. S. Workentin, *Chem.–Eur. J.*, 2008, **14**, 1698–1709.
6 R. L. Donkers and M. S. Workentin, *J. Am. Chem. Soc.*, 2004, **126**, 1688–1698.
7 D. L. B. Stringle and M. S. Workentin, *Chem. Commun.*, 2003, 1246–1247.
8 R. L. Donkers, J. Tse and M. S. Workentin, *Chem. Commun.*, 1999, 135–136.
9 Z. V. Todres, *Organic Ion Radicals: Chemistry and Applications*, Marcel Dekker, New York, 2003.
10 F. Maran, D. D. M. Wayner and M. S. Workentin, *Adv. Phys. Org. Chem.*, 2001, **36**, 85–166; F. Maran, D. D. M. Wayner and M. S. Workentin, in *Kinetics and Mechanism of the Dissociative Reduction of C–X and X–X Bonds (X = O, S)*, ed. T. T. Tidwell and J. P. Richard, New York, 2001.
11 J. M. Tanko and J. P. Phillips, *J. Am. Chem. Soc.*, 1999, **121**, 6078–6079.
12 J. P. Stevenson, W. F. Jackson and J. M. Tanko, *J. Am. Chem. Soc*, 2002, **124**, 4271–4281.
13 M. Chahma, X. Li, P. Phillips, P. Schwartz, L. E. Brammer, Y. Wang and J. M. Tanko, *J. Phys. Chem. A*, 2005, **109**, 3372–3382.
14 J. M. Tanko, X. Li, M. Chahma, W. F. Jackson and J. N. Spencer, *J. Am. Chem. Soc.*, 2007, **129**, 4181–4192.
15 R. L. Donkers and M. S. Workentin, *Chem.–Eur. J.*, 2001, **7**, 4012–4020.
16 R. L. Donkers and M. S. Workentin, *J. Phys. Chem. B*, 1998, **102**, 4061–4063.
17 M. S. Workentin and R. L. Donkers, *J. Am. Chem. Soc.*, 1998, **120**, 2664–2665.
18 M. G. Zagorski and R. G. Salomon, *J. Am. Chem. Soc.*, 1980, **80**, 2501–2503.
19 R. G. Salomon, *Acc. Chem. Res.*, 1985, **18**, 294–301.
20 D. J. Coughlin and R. G. Salomon, *J. Am. Chem. Soc.*, 1977, **99**, 655–657.
21 R. G. Salomon and M. F. Salomon, *J. Am. Chem. Soc.*, 1977, **99**, 3501–3503.
22 D. J. Coughlin, R. S. Brown and R. G. Salomon, *J. Am. Chem. Soc.*, 1979, **101**, 1533–1539.
23 B. S. Furniss, A. J. Hannaford, P. W. G. Smith and A. R. Tatchell, *Vogel's Textbook of Practical Organic Chemistry - 3-Benzoylpropanoic Acid*, John Wiley & Sons, New York, 1989.
24 K. Gollnick and G. O. Schenck, in *1,4-Cycloaddition Reactions*, ed. J. Hamer, Academic Press, New York, 1967, pp. 255–343.
25 Y. Takahashi, K. Wakamatsu, S. Morishima and T. Miyashi, *J. Chem. Soc., Perkins. Trans. 2*, 1993, 243–253.
26 W. Adam and H. J. Eggelte, *J. Org. Chem.*, 1977, **42**, 3987–3988.
27 J.-M. Savéant, in *Advances in Electron Transfer Chemistry*, ed. P. S. Mariano, Greenwich, 1994, vol. 4, pp. 53–116.
28 J.-M. Savéant, *Adv. Phys. Org. Chem.*, 2000, **35**, 117–192.
29 J. C. Imbeaux and J.-M. Savéant, *J. Electroanal. Chem.*, 1973, **44**, 169–187.
30 J.-M. Savéant and D. Tessier, *J.Electroanal. Chem. Interfacial Electrochem.*, 1975, **61**, 251–263.
31 D. D. M. Wayner and V. D. Parker, *Acc. Chem. Res.*, 1993, **26**, 287–294.
32 R. L. Donkers, F. Maran, D. D. M. Wayner and M. S. Workentin, *J. Am. Chem. Soc.*, 1999, **121**, 7239–7248.
33 The effective radius r_{eff} was calculated using the expression $r_{eff} = r_B(2r_{AB} - r_B)/r_{AB}$ where r_{AB} is the molecular radius, and r_B is the radius of the charged portion.[27] r_{AB} was determined from the Stokes–Einstein equation and the diffusion coefficient determined from the convolution experiments. r_B was approximated using the cumyl alkoxide anion.
34 C. Amatore, G. Capobianco, G. Farnia, G. Sandonà, J.-M. Savéant, M. G. Severin and E. Vianello, *J. Am. Chem. Soc.*, 1985, **107**, 1815–1824.
35 J.-M. Savéant, *Acc. Chem. Res.*, 1980, **13**, 323–329.
36 J. Pinson and J.-M. Savéant, *J. Am. Chem. Soc.*, 1978, **100**, 1506–1510.
37 S. E. Stein, R. L. Brown and Y. A. Mirokhin, in *NIST Standard Reference Database 25*, Gaithersburg, MD, 1991.
38 S. W. Benson, in *Thermochemical Kinetics: Methods for Estimation of Thermochemical Data and Rate Parameters*, ed. John Wiley and Sons Ltd., New York, 1976.
39 W. Adam, *Acc. Chem. Res.*, 1979, **12**, 390–396.
40 D. V. Avila, C. E. Brown, K. U. Ingold and J. Lusztyk, *J. Am. Chem. Soc.*, 1993, **115**, 466.
41 F. Najjar, C. André-Barrès, C. Lacaze-Dufaure, D. C. Magri, M. S. Workentin and T. Tzèdakis, *Chem.–Eur. J.*, 2007, **13**, 1174–1179.
42 P. M. O'Neill, P. A. Stocks, M. D. Pugh, N. C. Araujo, E. E. Korshin, J. F. Bickley, S. A. Ward, P. G. Bray, E. Pasini, J. Davies, E. Verissimo and M. D. Bachi, *Angew. Chem., Int. Ed.*, 2004, **43**, 4193–4197.
43 N. L. Drake and J. R. Adam, *J. Am. Chem. Soc.*, 1939, **61**, 1326–1329.
44 L. G. Greifenstein, J. B. Lambert, R. J. Nienhuis, G. E. Drucker and G. A. Pagani, *J. Am. Chem. Soc.*, 1981, **103**, 7753–7761.

This journal is © The Royal Society of Chemistry 2008

Org. Biomol. Chem., 2008, **6**, 3354–3361 | 3361